OPTIMIZATION OF SINGLE AND DUAL SUPPRESSORS UNDER VARYING LOAD AND PRESSURE CONDITIONS

Elliott R. Gruber[1], Kenneth A. Cunefare[1], Per W. Danzl[2], Kenneth A. Marek[1] and Michel A. Beyer[2]

[1]George W. Woodruff School of Mechanical Engineering, Georgia Institute of Technology, 771 Ferst Dr, Atlanta, GA 30332, USA
[2]Eaton Corporation, 7945 Wallace Road, Eden Prairie, MN 55344, USA
e_gruber@gatech.edu, ken.cunefare@me.gatech.edu, perwdanzl@eaton.com, ken.marek@gatech.edu, michelabeyer@eaton.com

Abstract

Hydraulic systems that operate over a broad range of load pressures pose challenges for suppression of fluid-borne noise. A common type of noise control device, a bladder-style suppressor, performs well only over a relatively narrow range of load or system pressures. This paper considers the problem of finding the optimal charge pressure(s) in either a single suppressor or two suppressors in series for maximum fluid-borne noise suppression in a weighted sense. The transmission loss, a measure of pressure ripple (dynamic pressure fluctuation) reduction, for the suppressors is predicted by an equivalent fluid model. The optimum configuration is sought through maximization of an objective function. The objective function is a summation of weighted transmission losses, where the weighting captures the duty cycle of the load pressure through a time weighting factor, and frequency weighting factor captures the spectral content of the pressure ripple. The duty-cycle weighting biases the objective function toward the most-used pressures. The frequency weighting emphasizes the high-energy spectral components in the target pressure ripple at a given load or system pressure. Optimal configurations are found for a set of system pressures, load pressures and duty cycles. It is found that the time weighting has a more significant impact on the optimum charge pressure than the frequency weighting, as seen by duty cycles considered in this paper.

Keywords: bladder-style suppressor, fluid-borne noise, optimization

1 Introduction

Fluid power applications may be noisy, which is both uncomfortable and hazardous to work around and may be damaging to equipment. The noise is caused by fluctuations in flow rate, known as flow ripple, which couples with system components to produce a dynamic pressure ripple through the system Johnston and Edge (1991). The spectral content of the related pressure ripple is unique to each system and depends on the pump, valves, and other system components. The pressure ripple may damage systems by exposing sealing surfaces to strong pressure pulses causing leaks, and system components are subject to additional stress cycles causing fatigue. The noise generated from the pressure ripple can be separated into three categories: fluid-borne noise (FBN), structure-borne noise (SBN) and air-borne noise (ABN) as noted by Johnston and Edge (1991). Their work also remarked that FBN-causes SBN and ABN, thus, suppressing FBN suppresses the other noise sources making the work environment more comfortable and the system less prone to failure. This work is concerned with the optimization of a passive control technique for a given set of operating conditions to reduce FBN.

Some devices currently used in practice to suppress FBN are Helmholtz resonators, side-branch resonators, expansion chambers and bladder-style suppressors. These types of noise control devices are compared using transmission loss (*TL*), which is the ratio of transmitted to incident acoustic energy; higher *TL* indicates better performance. A device exhibiting high *TL* prevents acoustic energy from propagating downstream, coupling with system elements and to predict noise control performance, methods for modeling Helmholtz resonators and side-branch resonators can be found in Kinsler, Frey et al. (1999). The modeling techniques allow for prediction of the resonant frequency and the *TL* curve of a resonant device with a rigid wall assumption. Both resonant devices exhibit high *TL* only in a narrow frequency band. To maximize *TL*, research has been performed to optimize quarter wave resonators (Okamoto et al., 1994)

This manuscript was received on 06 December 2012 and was accepted after revision for publication on 09 July 2013

using active control, however; active control is outside the scope of this work which focuses on the optimal condition of passive noise control techniques. Both the Helmholtz resonator and quarter wave resonator are placed perpendicular to flow, while expansion chambers are placed in-line with flow and exhibit better *TL* performance over a broad range. Marek et al., (2013) developed a method for predicting *TL* for a hydraulic expansion chamber based on a method for airborne expansion chambers by Selamet and Ji (1999). *TL* can be increased for an expansion chamber over the full range of frequencies without increasing dimensions by using a compliant liner. An example of a commercially available device with a complaint liner is bladder-style suppressors (Arendt, 1988). This device uses a pressurized volume of gas, most often nitrogen, as the complaint liner to reduce downstream pressure ripple, as described in Wilkes (1995). A traditional bladder-style suppressor has an inlet and outlet port, a bladder to separate the nitrogen gas from the hydraulic fluid, a perforated annulus to support the bladder when the system is not pressurized, as well as other components which are assumed to be acoustically insignificant. The bladder, annulus and flow path are coaxial. Bladder-style suppressors can exhibit *TL* near 30 dB over the frequency range of interest. Varying the bladder pressure, or “charge pressure”, varies the performance. For maximum performance, one manufacturer of bladder-style suppressors, Wilkes and McLean, advises to charge a suppressor to 50 % of system pressure. A report conducted by AlliedSignal Aerospace Equipment Systems of Tempe, AZ on behalf Wilkes and McLean, suggests that charging a suppressor to 60 % of system pressure is optimal. However, the work presented here as well as measurements of suppressor *TL* indicate that charging the suppressor to 90 % of system pressures yields the highest *TL*. Based on the work of Marek et al., (2013), it can be seen a higher charge pressure is beneficial because the acoustic impedance change at the suppressor is greater. Any impedance change will cause some energy to be reflected, preventing its transmission downstream. A larger impedance change reflects more energy therefore a greater charge pressure is desirable. However, a charge pressure which is greater than system pressure causes the impedance change to drastically reduce, lessening the effectiveness of the suppressor. The *TL* experiments were conducted at a single system pressure, yet fluid power equipment is used over a range of pressures. It has also been observed that a suppressor charged to equal or greater than system pressure yields much lower *TL* than a suppressor charged to less than system pressure for all frequencies of interest. Other than the recent work of Marek et al., (2013), there does not appear to be material in the literature that speaks to the performance of bladder-style suppressors, much less their optimization for a given application.

There is a need to determine the charge pressure of bladder-style suppressors that yields the optimal noise control performance, in some sense, in the presence of time-varying system pressures. This paper presents an optimization approach using an analytical model of bladder-style suppressor performance as well as information pertaining to an applications load-pressure time history and pressure ripple at those load pressures. The approach uses an objective function that weights the *TL* by a frequency-weighting factor and time-weighting factor to determine optimal charge pressure configurations. The approach may be applied to single suppressors or to configurations of two suppressors in series. The motivation for considering configurations in series is driven by some applications that are in development with particularly demanding pressure ripple and fluid-borne noise environments.

2 Optimization and Objective Function

The optimization procedure considered here uses a direct-search approach to determine the optimal charge pressure in bladder-style suppressors. The objective function for the optimization represents a weighted sum of predicted transmission loss for a given single or dual in series suppressor configuration. The predicted *TL* of the suppressor(s) is obtained using an analytical model, developed by Marek et al., (2013). The model treats the bladder as an equivalent fluid and solves the eigenvalue problem for the wave modes in the up- and downstream pipes, and in both the fluid and nitrogen within the suppressor. The model is explained in further detail in the paper by Marek et al., (2013). The frequency weighting factor (FWF) weights the objective function with the spectral content of the pressure ripple, and the time weighing factor (TWF) weights the objective function with the duty cycle of system pressures. The FWF and TWF are relevant to a given application or work cycle, and may be determined from measurements on the system of interest to ensure best performance for that system and work cycle. An optimal charge pressure configuration is defined by the charge pressure configuration which maximizes the objective function. The development of the objective function is described below, as well as the individual effects of the FWF and TWF.

The objective function considered here is applicable to a system using either one suppressor or two suppressors in series. The optimal charge pressure condition is found by maximizing the objective function

$$\mathfrak{F}(p_{c,1}, p_{c,2}) = \frac{1}{|U|} \sum_{(i,j,k)\in U}^{N} |D_i| \frac{1}{|\Omega|} \cdot \sum_{\omega\in\Omega}^{M} |W_i(f)| \cdot |TL(f, p_{s,i}, p_{c,j}, p_{c,k})| \quad (1)$$

where the optimal charge pressure condition is defined by

$$(p_{c,1}, p_{c,2})^* = \arg\max_{p_{c,1}, p_{c,2}} \mathfrak{F}\left(p_{c,1}, p_{c,2}\right) \quad (2)$$

In Eq. 1, *TL* is the predicted transmission loss of the suppressor, *f* is the frequency in Hertz over Ω (the frequency bandwidth of interest), $p_{\mathrm{s,i}}$ is the system or load pressure, $p_{\mathrm{c,j}}$ and $p_{\mathrm{c,k}}$ are the charge pressures for two suppressors. The system pressure and both charge pressures belong to the set, *U* the pressure range of interest. If the optimization is being using for a single suppressor, then only $p_{\mathrm{c,j}}$ is used in Eq. 1. Weighting factors *D* and W, described in more detail below, capture time-dependent aspects of the load pressure, and spectral content of the pressure ripple, respectively. The frequency range of interest, the range of charge and static pressures considered for this paper are shown in Table 1.

Table 1: Frequency range and pressures used in this study

Parameter	Value
Frequency	10 - 5200 Hz
Charge Pressure, p_c	3.45 - 20.7 MPa
System Pressure, p_s	0.690 - 20.7 MPa

The spectral content of a given pressure ripple will depend upon how it was generated. For example, the pressure ripple due to positive displacement pumps will be comprised of frequency components dominated by the pumping element frequency and its harmonics; the magnitude of the pressure ripple and its spectral content may depend on the load pressure. It is desirable to ensure that the suppressor performance targets these dominant spectral components. This is accomplished through the use of a frequency-weighting factor W in the objective function, defined as

$$W_i(f) = \frac{|P_{d,i}(f)|}{\max\limits_{\omega,i} |P_{d,i}(f)|} \tag{3}$$

where $|P_{d,i}(f)|$ is the magnitude of the dynamic pressure ripple at the i^{th} system pressure.

A fluid power application may spend different amounts of time at different load pressures; each load pressure may have different pressure ripple conditions. To account for this time dependency, a time weighting factor D is incorporated into the objective function, and is defined as

$$D_i = \frac{t_i}{t_{total}} \tag{4}$$

where t_i is the amount of time the system spends at the i^{th} system pressure, and t_{total} is the total time in a complete duty cycle.

The TL is itself directly dependent on the optimization variables, $p_{c,j}$ and $p_{c,k}$. The calculation of TL is described in the following section.

2.1 Transmission Loss

For a bladder-style suppressor, TL is a function of its geometrical dimensions shown in Fig. 1. Critical dimensions include the inner radius of the inlet and outlet ports, r_{port}, the outer radius of the annulus, $r_{annulus}$, the inner radius of the shell, r_{shell}, and the effective internal length of the device, L. The other components are assumed to be acoustically insignificant. In addition to the geometric properties, TL is also dependent on the nitrogen charge pressure and system pressure. Higher TL can be achieved with a two suppressor setup, shown in Fig. 2, which has an additional dimension, separation distance, S, affecting TL, due to standing wave behavior in the connecting section of pipe between the suppressors.

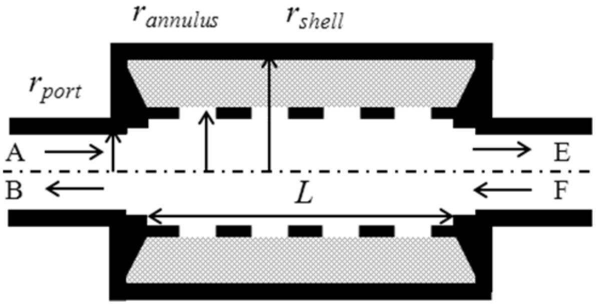

Fig. 1: *Single Suppressor Dimensions and Acoustic Waves*

An equivalent fluid model is used to calculate the wavefields associated with a single suppressor. The development and validation for the model can be found in Marek et al., (2013). Marek discusses the calculation of acoustic waves in the pipes, shown as waves A-F in Fig. 1 and Fig. 2, as well as the acoustic behavior within the suppressor(s). The waves are calculated from simultaneously solving series of pressure and particle displacement relations and applying boundary conditions relevant to the suppressor. The single suppressor model of Marek et al., (2013) was modified for the work at hand to simulate a two suppressor configuration. The labels A through F in Fig. 1 and Fig. 2 designate the complex wavefield amplitudes in the relevant portions of the suppressor configuration. The complex wave amplitudes are used to calculate TL using the equation found in Earnhart et al., (2010),

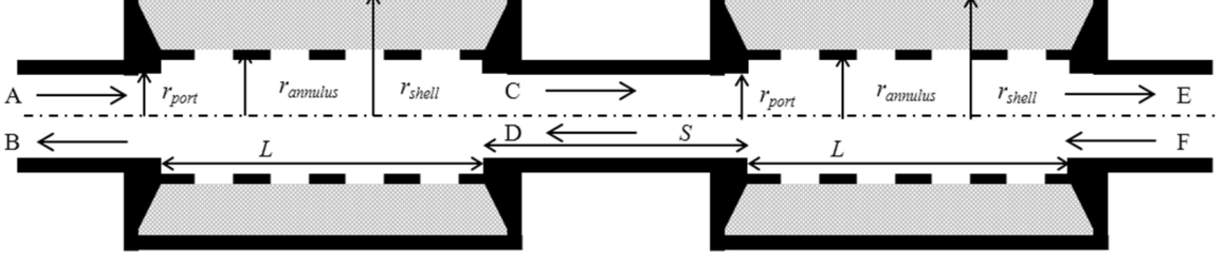

Fig. 2: *Double Suppressor Dimensions and Acoustic Waves*

$$TL = 20\log_{10}\left|\frac{A^2 - F^2}{AE - BF}\right| \tag{5}$$

Equation 5 differs from the usual form of *TL*, as it accounts for a coherent reflected wave component *F* in the downstream section; if the downstream section is terminated anechoically, as assumed in the model presented by Marek and used here, then the expression for *TL* reduces to the more familiar form

$$TL = 20\log_{10}\left|\frac{A}{E}\right| \tag{6}$$

Using the model developed by Marek et al., (2013), the predicted *TL* for a bladder style suppressor with dimensions seen in Table 2, operating at 20.7 MPa is shown in Fig. 3, for a range of single charge pressures in a single suppressor system, and Fig. 4, for a range of charge pressure pairs in a double suppressor system, revealing that increasing charge pressure of the suppressors increases *TL* until the charge pressure is greater than or equal to the system pressure. Figure 4 shows if one suppressor of a pairing is over–charged (charge pressure greater than system pressure), *TL* performance significantly decreases, to that of a single suppressor. The suspected cause of significantly lower performance exhibited by overcharged suppressors is that the bladder remains in contact with the annulus, thus the suppressor behaves similar to an expansion chamber instead of a bladder-style suppressor. Note that the very high *TL* predicted for the dual suppressor configuration, Fig. 4, may not be achievable in practice due to other paths for an excitation to take past a suppressor; measurement of such high *TL*s may also be problematic as the signal dips below the noise floor of the transducer.

Table 2: Dimensions of Bladder-style Suppressor used in this study

Parameter	Value
r_{port}	0.0176 m
$r_{annulus}$	0.0252 m
r_{shell}	0.0417 m
L	0.0682 m
S	0.10 m

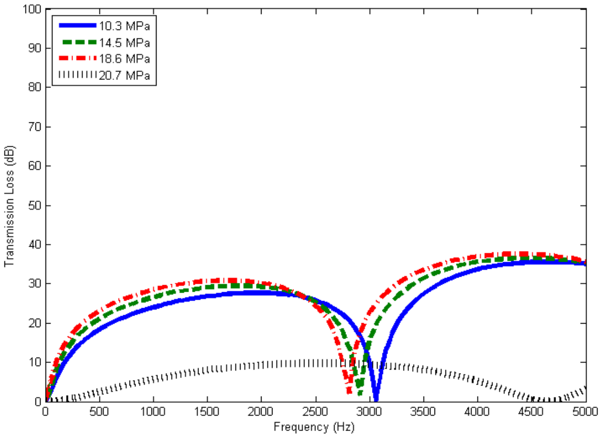

Fig. 3: *Single suppressor system TL at 20.7 MPa system pressure with varying charge pressures*

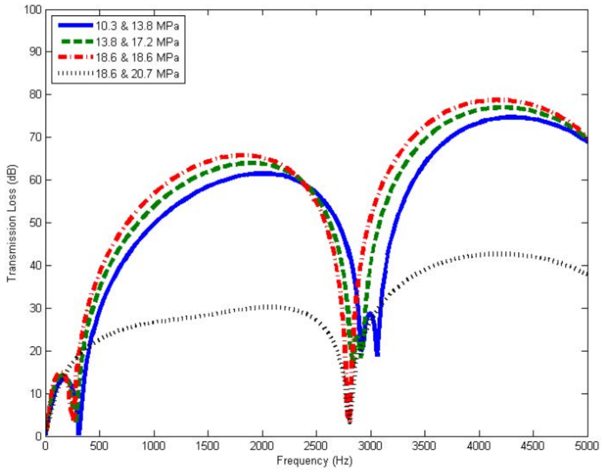

Fig. 4: *Double suppressor system TL at 20.7 MPa system pressure with varying charge pressures Frequency Weighting Factor*

The objective function is frequency-weighted to account for variation in energy density over the frequency band of interest using the FWF, Eq. 3. The spectral content of the pressure ripple in a given hydraulic system is due to a variety of factors, including the choice of pump, valves and line lengths in the system. To weight different pressure ripples consistently, the frequency content of the pressure ripple assumed incident on the suppressor is normalized to the maximum pressure ripple amplitude at all load pressures under considerations. This yields a maximum FWF of 1 at the frequency of maximum pressure ripple among all ripples at each load pressure. The FWF at all other frequencies and load pressures will have a value between 0 and 1, depending upon the shape of the pressure ripple spectrum. Using the FWF ensures frequencies with low acoustic energy are ignored while frequencies with high energy will contribute significantly to the objective function value.

An example set of FWFs for four load pressures, shown in Fig. 5, was generated from data measured on a test fixture at Eaton. The test fixture implemented the method for measurement of fluid borne noise embodied in ISO-15086-1 (2001), with the data averaged over multiple tests. Flow was supplied to the test fixture by a 9-piston axial pump operating at 1500 rpm. Note that the FWF weights the input noise signal, no matter what the specific source of that signal (e.g., it is not dependent on a specific pump type or rotation speed). With the exception of the 240 Hz component at the 13.8 MPa load pressure, Fig. 5c, generally, higher system pressures have a higher magnitude of FWF reflecting increased magnitude of pressure ripple with increasing load pressure.

The objective function is weighted to the most-used load pressures using the TWF, Eq. 4. In practice, hydraulic system duty cycles typically encompass a broad range of load pressures with unequal time spent at each load pressure. As noted earlier, load pressure affects both *TL* and FWF, thus, the amount of time the system spends at each pressure needs to be accounted for in the objective function. The TWF is the time fraction of each load pressure relative to some user-defined complete work cycle. Longer usage at a given load pressure will bias the objective function towards those load pressures.

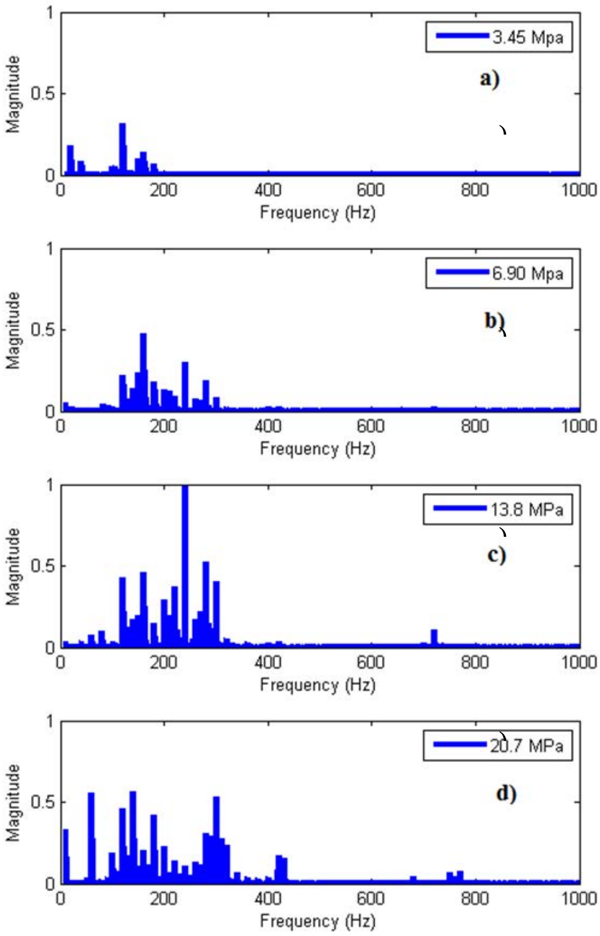

Fig. 5: *Frequency weighting factor (FWF) for system pressures of: a) 3.45 MPa, b) 6.90 MPa c) 13.8 MPa d) 20.7 MPa Time Weighting Factor*

Two cases of TWFs are shown in Fig. 6 and Fig. 7. Case 1, depicted in Fig. 6, represents a system that operates at 20.7 MPa for 5 % of its duty cycle and 13.8 MPa for over 50 % of its duty cycle. The TWF for Case 2, depicted in Fig. 7, represents a system that operates at 20.7 MPa for 45 % of its duty cycle at 20.7 MPa, and operates at 6.90 and 13.8 MPa for approximately 25 % of its duty cycle at each pressure. The TWFs only have values for the matching system pressures, an approximation made for this work. The system pressures for a real system will have a continuous distribution instead of the discrete pressures shown. The TWFs shown in this work are representative of the boom pressure on a hydraulic excavator working in a pond dredging application, TWF Case 1 shown in Fig. 6, and a pit digging application, TWF Case 2 shown in Fig. 7.

A hydraulic system may be used in different ways with different duty cycles. Recharging the suppressors for each duty cycle is time consuming and impractical. To account for this, the TWF can represent more than one duty cycle, instead representing the total usage between scheduled recharges. The sum of the TWF across all load pressures in the optimization is 1, representing a complete cycle.

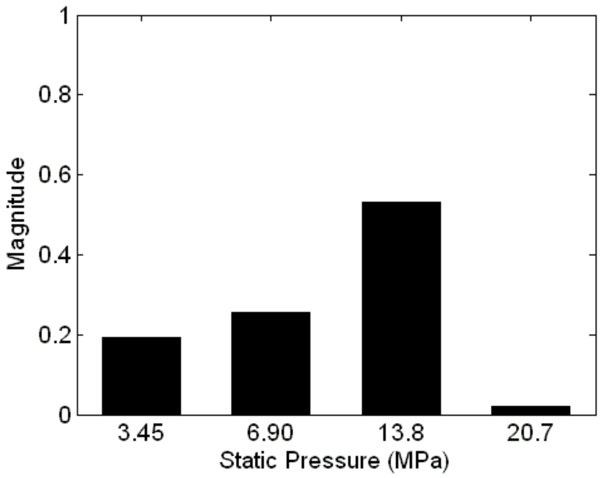

Fig. 6: *Case 1 TWF*

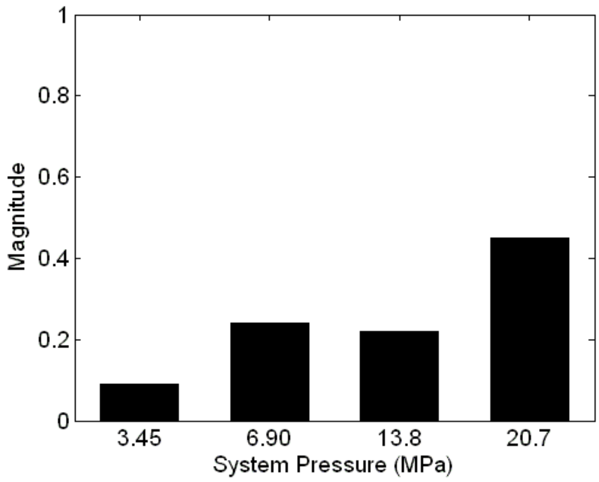

Fig. 7: *Case 2 TWF*

3 Example Optimization for Single Suppressor

The objective function was computed for a single suppressor, requiring the predicted *TL* for all combinations of the charge pressure and system pressure values in Table 1, the FWFs shown in Fig. 5, and the two cases of TWFs shown in Fig. 6 and Fig. 7. The values of the objective function for Case 1 over the charge pressure range are shown in Fig. 8. The charge pressure value with the global optimum for the objective function is 13.1 MPa; however, a local optimum occurs at 6.21 MPa with an objective function value of over 99 % of the global optimum, which is a statistically insignificant difference. Both points are the single pressure optimum, i.e. optimal charge pressure for a system operating at a single pressure. A single pressure optima is a charge pressure which causes the suppressor to exhibit the highest *TL* for a given system pressure. The single pressure optima is found to be a charge pressure of 90 % of system pressure. In order to differentiate between the optimal charge pressures for this case, aspects not captured by the objective function are considered. The first aspect is the slope of the objective function. The charge pressure of the suppressor decreases over time because of imperfect sealing of the nitrogen and permeation of nitrogen through the bladder. For Fig. 8, the slope of the objective near the charge pressure of 13.1 MPa is more gradual; therefore charging to this condition would provide a more robust configuration as it would not need recharging as quickly. Another aspect not directly captured by the objective function to consider is the coupling of FBN to ABN in the system, as one secondary goal is to reduce ABN. The relationship between FBN and ABN is difficult to predict, and as such this aspect must be measured in the field or modeled using a finite-element modeling/boundary element modeling approach.

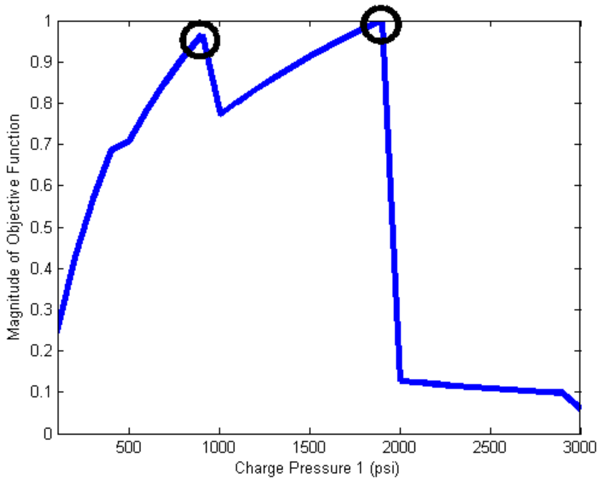

Fig. 8: *Normalized Objective Function Values Case 1 for Single Suppressor. Circles indicate local optima at 6.21 MPa and 13.1 MPa*

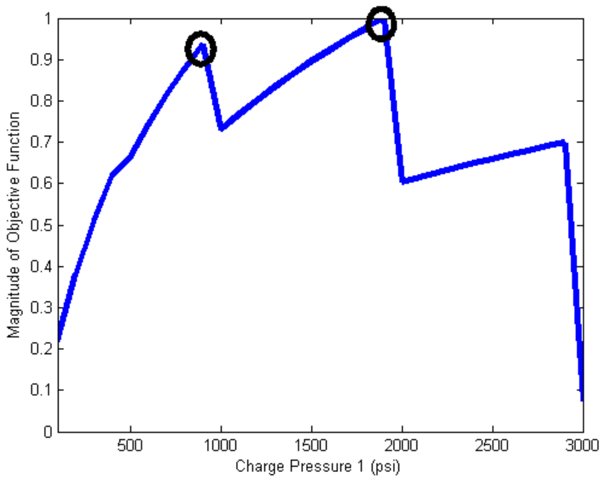

Fig. 9: *Objective Function Values Case 2 for Single Suppressor. Circles indicate local optima at 6.21 MPa and 13.1 MPa*

The objective function was computed again for a single suppressor with the second TWF case. The values of the objective function for this case are shown in Fig. 9. The charge pressure value with the global optimum of objective function is 13.1 MPa; however, as in Fig. 8, a local optimum occurs at 6.21 MPa with a value over 94 % of the global optimum, and should be considered as a potential optimal condition. The same aspects used to differentiate between the optimal charge pressures, and the charge pressure of 13.1 MPa is more robust and therefore the optimal condition. Both Case 1 and Case 2 required analysis of aspects not captured by the objective function.

The effect of the TWF shown in Fig. 7, can also be studied using the results shown in Fig. 9. The largest TWF value in Case 2 occurs at 20.7 MPa. This may lead to the assumption that the global optimum should be the single pressure optimum for 20.7 MPa. As presented in Fig. 9, a local optimum occurs at a charge pressure of 20.0 MPa, corresponding to the optimum charge pressure for the 20.7 MPa system pressure if it was present 100 % of the time, but this is not the global optima. The reason the 20.0 MPa charge pressure is not the optimal condition is due to similarities in the FWF for the 13.8 and 20.7 MPa system pressure as seen in Fig. 4 and Fig. 5. The FWF for 20.7 MPa system pressure is only slightly higher than the FWF for 13.8 MPa system pressure. In addition, overcharged suppressors exhibit low *TL* which lowers the objective function value for the corresponding charge pressures; the fact that the example system spends significant time at lower system pressures leads to a significant amount of time where the suppressor would be overcharged. The inverse condition is not true: the optimal condition for the low system pressure does not perform optimally for higher system pressure, but performs better than overcharged suppressors for the same system pressure.

4 Example Optimization for Dual In-line Suppressors

The objective function was computed for a pair of suppressors over the full design space, which includes all *TL* combinations predicted from the charge pressure and system pressure values in Table 1, the FWFs shown in Fig. 5, and the two cases of TWFs shown in Fig. 6 and Fig. 7. The values of the objective function for Case 1 over the range of charge pressure pairings are shown in Fig. 10. The maximum value of the objective function occurs at a charge pressure pairing of 2.07 and 13.1 MPa. The large dark region, where both suppressors are charged over 13.8 MPa, represents very low objective function values. This result is expected as this charge pressure region is only exhibits high *TL* for a system pressure of 20.7 MPa, and Case 1 only spends 2 % of its TWF at this pressure. Several local optima above 90 % of optimal objective function value are also seen in Fig. 10 at charge pressure pairings of: 6.21 and 13.1 MPa, 13.1 and 13.1 MPa and 2.76 and 6.21 MPa. These pairings may also be valid choices for practical usage, aspects not captured by the objective function must be considered to determine the optimal condition. The first aspect is the gradient of the objective function near the local optimum, since the charge pressure of the suppressor decreases over time because of imperfect sealing of the nitrogen and diffusion of nitrogen through the bladder. For Fig. 10, a charge pressure pairing of 2.07 and 13.1 MPa exhibits the smallest gradient in its respective region and is the optimal charge pressure configuration for a double suppressor simulation for the TWF shown in case 1. With the exception of a charge pressure of 2.07 MPa, all charge pressures involved with local optima pairings are single pressure optima, i.e. optimal charge pressure for a system operating at a single pressure with a single suppressor. A charge pressure pair of 2.76 and 13.1 MPa has a value over 99.9% of the optimal value, which is statistically insignificant. The difference can be attributed the *TL* of a charge pressure pairing of 2.07 and 13.1 MPa exhibiting higher *TL* than a charge pressure pair of 2.76 and 13.1 MPa in frequencies with high FWF values, seen in Fig. 5. If a charge pressure pair of 2.76 and 13.1 MPa replaces the charge pressure pair of 2.07 and 13.1 MPa as the local optima, all local optima charge pressures are found to be single pressure optima.

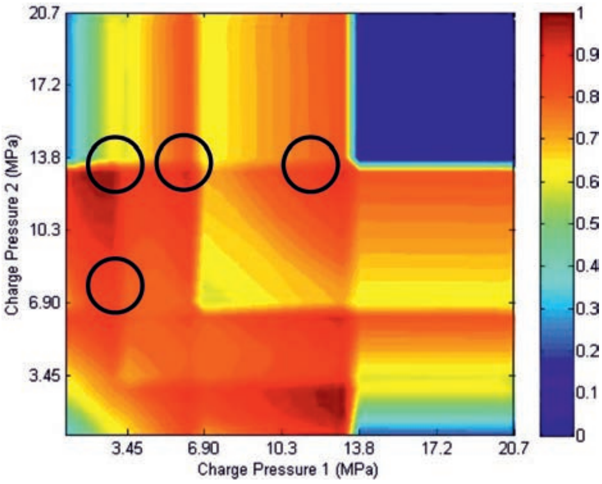

Fig. 10: *Normalized Objective Function values for Case 1 for Double Suppressors. Circles indicate charge pressure pairings of 2.07 and 13.1 MPa, 6.21 and 13.1 MPa, 13.1 and 13.1 MPa and 2.76 and 6.21 MPa*

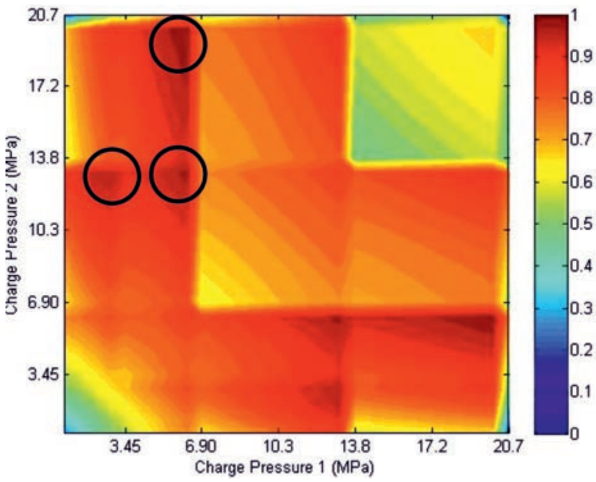

Fig. 11: *Normalized Objective Function Values for Case 2 for Double Suppressors. Circles indicate charge pressure pairings of 6.03 and 20.0 MPa, 2.76 and 13.1 MPa and 6.21 and 13.1 MPa*

The objective function was computed again using the same *TL* data and same FWF, but with the TWF representing Case 2 presented in Fig. 7. The highest value of the objective function is 6.03 and 20.0 MPa. Two local optima, charge pressure pairings of 2.76 and 13.1 MPa and 6.21 and 13.1 MPa, have values over 90 % of the highest objective function value. Again, the gradient of these points are considered to differentiate which charge pressure pair should be selected. The optimal charge pressure pairing for Case 2 TWF, shown in Fig. 7, is a charge pressure pair of 6.03 and 20.0 MPa. All charge pressure pairings yielding local optima for the Case 2 TWF are pairings of single pressure optimum.

The effect of TWF can be seen when comparing Fig. 10 and Fig. 11, as the only difference is which TWF case is applied. The local optimal for both TWF cases share similar charge pressure pairings. The charge pressures in these pairings are often combinations the single pressure optimum; the overall optimum and relative magnitude of the local optima are determined by the TWF applied.

5 Conclusions and Future Work

An optimization procedure to determine the charge pressure condition for both one and two suppressor systems has been developed for a system operating with an arbitrary flow source and duty cycle. For a one suppressor system, the global optimum charge pressure and next highest local optimum charge pressure are very close for both conditions evaluated. This requires aspects not captured by the objective function to be used to select the optimal charge pressure. For a two suppressor system, most predicted optimal conditions are made up of single pressure optima, rarely the FWF may cause a non-single pressure optima to yield the optimal charge pressure pairing. Comparing the two suppressor optimization for both TWF cases shows the dependency of the optimal points on the TWF being used.

Future work will include measuring more FWFs for a given system to have increased resolution between simulated charge pressures. FWFs measured on a different system would allow for a more in-depth look at the effect the FWF has on the optimal condition. In addition, greater system pressure resolution for the FWF will allow the TWF to better represent actual system usage. In a practical application system pressure often drifts or oscillates. In order to investigate the effect varying system pressure may have on the optimal condition(s), the gradient of the objective function as a function of system pressure would be analyzed. Validation will be conducted to verify optimal conditions perform as predicted. In addition, future work may include simulating non-identical suppressors for the suppressor pair. This optimization routine can be used to select geometric and material parameters of future suppressor designs.

Acknowledgements

The authors would like to thank Eaton Corporation for funding this work.

Nomenclature

A, B, C, D, E, F	Acoustic wave amplitudes	[Pa]
D_i	Time weighting factor of *i* system pressure	[ND]
f	Frequency	[Hz]
L	Length of Suppressor	[m]
p_c	Charge pressure	[Pa]
p_s	System Pressure	[Pa]
$r_{annulus}$	Radius of suppressor annulus	[m]
r_{port}	Radius of suppressor port	[m]
r_{shell}	Radius of suppressor shell	[m]
S	Separation distance of Suppressors	[m]
TL	Transmission Loss	[dB]
U	Range of Pressures	[Pa]
W_i	Frequency Weighting factor of *i* system pressure	[ND]
Ω	Frequency Band	[Hz]

References

Arendt, E. 1988. Pulsation Absorbing Device, in: USPTO, Wilkes-McLean, Ltd., United States.

Earnhart, N. E., **Marek, K. A.** and **Cunefare, K. A.** 2010. Evaluation of hydraulic silencers, *NoiseCon10*. Baltimore, MD.

ISO-15086-1 2001. Hydraulic fluid power - Determination of fluid-borne noise characteristics of components and systems - Introduction. Geneva, Switzerland.

Johnston, D. N. and **Edge, K. A.** 1991. A Test Method for Measurement of Pump Fluid-Borne Noise Characteristics, *International Off-Highway & Powerplant Congress and Exposition*. Milwaukee, Wisconsin.

Kinsler, L. E., **Frey, A. R.**, **Coppens, A. B.** and **Sanders, J. V.** 1999. *Fundamentals of Acoustics*. 4th ed. John Wiley & Sons, Inc.

Marek, K. A., **Gruber, E. R.** and **Cunefare, K. A.** 2013. Linear Analytical Model for a Pressurized Gas Bladder Style Hydraulic Silencer. *International Journal of Fluid Power*, Vol. Submitted, pp.

Okamoto, Y., **Bodén, H.** and **Åbom, M.** 1994. Active noise control in ducts via side-branch resonators. *Journal of the Acoustical Society of America*, Vol. 96, pp. 1533-1538.

Selamet, A. and **Ji, Z. L.** 1999. Acoustic Attenuation Performance of Circular Expansion Chambers With Extended Inlet/Outlet. *Journal of Sound and Vibration*, Vol. 223, pp. 197-212.

Wilkes, R. G. 1995. Reduction of Noise in Hydraulic Systems. *SAE Technical Paper 952154*, Vol. pp.

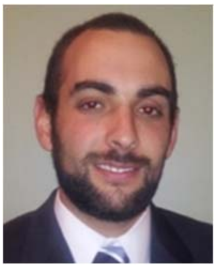

Elliott Gruber
earned a BSME degree from the Georgia Institute of Technology in 2007. He is currently pursuing a Ph. D. in Mechanical Engineering, also at the Georgia Institute of Technology.

Dr. Kenneth Cunefare
is a Professor at the Georgia Institute of Technology. He began at Georgia Tech in 1990. Prior he was the F.V. Hunt Postdoctoral Fellow at The Technical University of Berlin. He earned his PhD in 1990 from the Pennsylvania State University. He is currently Professor in Charge of the Integrated Acoustics Laboratory.

Dr. Per Danzl
is with the Eaton Innovation Center and specializes in control system design, signal processing and analysis. He is a member of the Control Systems and Solutions group, focusing on advanced control for hydraulic hybrid systems. He received a BSME from University of Minnesota ('02) and a Ph.D. in Mechanical Engineering from the University of California Santa Barbara ('10).

Kenneth Marek
has a BSME degree from Texas Tech University and is currently a Ph.D. candidate in Mechanical Engineering at the Georgia Institute of Technology. His research focuses on modeling and simulation of noise control technologies for fluid power.

Michel A. Beyer
is a senior engineering specialist at Eaton Corporation in Eden Prairie Minnesota as part of the Noise and Vibration Center of Excellence. He began his career at Cummins Engine Company in Columbus Indiana. He earned a B.S. in Mechanical Engineering at South Dakota State University and an M.S. in Engineering from Purdue University.